Chemical Engineering Journal 286 (2016) 408–415

Contents lists available at ScienceDirect

Chemical Engineering Journal

journal homepage: www.elsevier.com/locate/cej

Selective reduction of nitrate into nitrogen using Fe–Pd bimetallic nanoparticle supported on chelating resin at near-neutral pH

Jialu Shi [a], Chao Long [a,b,*], Aimin Li [a,b]

[a] State Key Laboratory of Pollution Control and Resource Reuse, School of the Environment, Nanjing University, 163 Xianlin Avenue, Nanjing 210023, China
[b] Nanjing University Yancheng Environmental Protection Technology and Engineering Research Institute, 888 Yingbin Road, Yancheng 22400, China

HIGHLIGHTS

- Bimetallic Fe–Pd nanoparticles were immobilized effectively onto resin DOW 3N.
- Loading order of Fe and Pd affected the activity and selectivity of DOW 3N-Fe/Pd.
- Nitrate removal (>95%) using DOW 3N-Fe/Pd was obtained at near-neutral pH.
- N_2 selectivity of 71.0% was obtained at pH 8.67 without addition of reductant H_2.

GRAPHICAL ABSTRACT

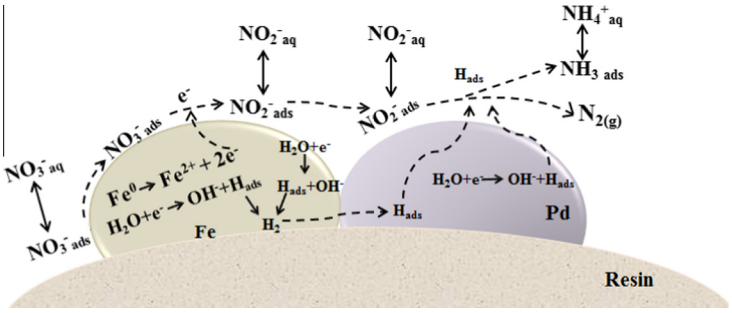

ARTICLE INFO

Article history:
Received 18 August 2015
Received in revised form 22 October 2015
Accepted 23 October 2015
Available online 2 November 2015

Keywords:
Nitrate removal
Selective reduction
Fe–Pd bimetallic
Chelating resin

ABSTRACT

Nano zero valent iron (nZVI) has emerged as a promising water treatment technology for reduction of contaminants. Unfortunately, for nitrate reduction by nZVI, near 100% of nitrate was converted to undesired ammonia (NH_3) and not to nontoxic nitrogen (N_2). In this study, supported bimetallic Fe–Pd nanoparticles were prepared by loading Fe and Pd on chelating resin (DOW 3N) by two different methods. The effect of the preparation method, solution pH and Pd loading on the reactivity and selectivity of Fe–Pd composites for nitrate removal was investigated at near-neutral pH in unbuffered solution. The results suggest that DOW 3N-Fe/Pd, which was prepared by loading Pd firstly and then Fe on DOW 3N, showed a remarkable nitrate removal (>95%). The selectivity to N_2 was increased with the increase of Pd content and solution pH; the N_2 selectivity of 69.2% was obtained at pH 6.75 using DOW 3N-Fe/Pd with 8 wt.% Pd–8 wt.% Fe. The high selectivity to N_2 benefited from the closer contact distance between Pd and Fe on the surface of DOW 3N-Fe/Pd and low intraparticle diffusion resistance.

1. Introduction

Excess NO_3^- in drinking water is a potentially harmful contaminant because it may cause adverse health effects to humans, such as blue-baby syndrome (methemoglobinemia) and cancer. The World Health Organization has set the maximum contaminant level for nitrate at 10 mg N L^{-1} in drinking water. Diverse technologies have been developed to treat the water contaminated by NO_3^-. Ideally, NO_3^- should be selectively reduced to N_2 without further reduction to NH_4^+. Biological denitrification, catalytic hydrogenation and photocatalytic reduction have been reported as the promising technologies for selectively reducing nitrate to nontoxic N_2. However, these technologies suffer from sludge generation or massive addition of chemicals such as H_2 and oxalic acid [1,2].

Nano zero valent iron (nZVI) has been intensively studied for reductive removal of nitrate from water [3–6]. However, nZVI

* Corresponding author at: State Key Laboratory of Pollution Control and Resource Reuse, School of the Environment, Nanjing University, 163 Xianlin Avenue, Nanjing 210023, China. Tel.: +86 25 89680380.
E-mail address: clong@nju.edu.cn (C. Long).

http://dx.doi.org/10.1016/j.cej.2015.10.054
1385-8947/

particles tend to agglomerate into large particles, leading to a lower removal efficiency and reactivity. Moreover, nitrate was mainly reduced into undesired ammonium as the primary end product [7,8]. So, several strategies had been developed to enhance nitrate reduction by nZVI, including (1) immobilization of nZVI on support materials [9,10] and (2) deposition of other metals such as Cu, Ni, Pd, onto nZVI surfaces [11–13]. Even though these approaches resulted in significant increases in the reduction of NO_3^-, the N_2 yields remained low without pH control. An optimum N_2 selectivity of 30% was obtained in alkaline solution (pH = 7.5–8.5) using the ZVI deposited bimetallic Pd and Cu [13]. Although it is reported that nitrate could be converted into nitrogen gas with maximum 66% selectivity by the stabilized nZVI with carboxymethyl cellulose at pH 7–7.5 with buffer solution, only 40% of nitrate was reduced without the addition of a buffer [14]. However, pH control with buffer solution is inconvenient and not practical. In addition, nitrate removal by adsorption of reactive iron hydroxides formed during the reduction was not considered in these studies, which had a significant contribution to nitrate removal [15]. Therefore, an effective method is required to remove nitrate by nZVI with high N_2 selectivity in near-neutral pH without buffer solution.

The support can have an indirect effect on activity and selectivity by influencing the density, size, morphology of metallic nanoparticles. Recently, we reported that the nZVI immobilized onto the chelating resin (DOWEX™ M4195) had a high removal efficiency for nitrate [16]; however, the main problem was that undesired ammonium was the primary end product at a yield of >82%. Numerous studies had demonstrated that the iron-based bimetallic particles could degrade contaminants faster than monometallic ZVI particles [17,18]. In general, Pd was more catalytic active than the other metals (Ni, Pt or Cu) [12,19] and had been proved to be the most selective for nitrite reduction [10]. In the present work, bimetallic Fe/Pd nanoparticles were immobilized in DOWEX™ M4195 for nitrate reduction with a high N_2 selectivity without buffered solution. The overall objective of this study is to investigate the effect of methods of preparation of supported nanoparticles, solution pH and Pd loading on the denitrification rate and N_2 selectivity, and to acquire further insights into the underlying nitrate reduction mechanism.

2. Materials and methods

2.1. Materials

DOWEX™ M4195 (DOW 3N) was purchased from Sigma–Aldrich. The physicochemical properties of DOW 3N was shown in Table S1. The resin is composed of a polystyrene cross-linked with divinyl benzene backbone and bis (2-pyridylmethyl) amine functional groups. Prior to use, the resin was extracted with ethanol in a Soxlet apparatus for 8 h, and then washed by 4 wt.% hydrochloric acid and 4 wt.% sodium hydroxide. All chemicals including ferric sulfate ($Fe_2(SO_4)_3$), palladium chloride ($PdCl_2$), ethyl alcohol, sodium borohydride ($NaBH_4$), sodium nitrate ($NaNO_3$) were of analytical grade and purchased from Nanjing Chemical Reagent Co. Ltd., China.

2.2. Preparation of supported nanoparticles

The typical synthesized procedure in the present study is depicted as follows: 1 g DOW 3N resin was added into 500 mL Fe^{3+} solution containing 2–3 g L^{-1} of Fe^{3+} and shaken for 24 h at 30 °C. Then, the resin spheres were added into 125 mL of 150–650 mg L^{-1} Pd^{2+} solution and shaken for 10 h at 30 °C. Afterwards, the resin spheres were reduced by 100 mL 2% $NaBH_4$ solution with constant stirring for 2 h at 20 °C under the N_2 atmosphere. The obtained product was called DOW 3N-Fe/Pd. Another method to prepare the supported bimetallic nanoparticles called DOW 3N-Fe/Pd-R was to load Pd firstly and then Fe. One gram of DOW 3N resin was added into 125 mL 650 mg L^{-1} Pd^{2+} solution and shaken for 10 h at 30 °C. Then the resin spheres were added into 500 mL Fe^{3+} solution containing 3 g L^{-1} of Fe^{3+} and shaken for 10 h at 30 °C. Finally, the resin spheres loaded with Pd and Fe were reduced by $NaBH_4$ using the same method with DOW 3N-Fe/Pd.

The amount of Fe and Pd loaded onto the DOW 3N was calculated by determining the initial and final concentrations of the preparation solution using an atomic absorption spectrophotometer (AA-6300C). In all cases, the Fe loading was approximately 80 ± 5 mg g^{-1} by changing the initial Fe^{3+} solution.

2.3. Characterization

The X-ray diffraction (XRD) analysis was performed by X-ray diffractometer (ARL X'TRA, Switzerland). High-resolution transmission electron microscope (HR-TEM) analyses were performed using electron microscope (JEM-2100, Japan). The Fe and Pd distribution in resin was observed by scanning electron microscope–energy dispersive spectrometer (SEM–EDS) (S-3400N II, Japan). The surface chemistry of NZVI was analyzed by X-ray photoelectron spectroscopy (XPS) (PHI5000 VersaProbe, Japan).

2.4. Batch experiments

All the batch experiments were carried out in three-neck flask at 25 °C. A certain amount of composites with various Pd loadings (2–8% in mass) were added to 500 mL of 20 mg N L^{-1} nitrate solution stirred with a mechanical stirrer, in which the content of Fe was kept at about 160 mg L^{-1}. Nitrate solution was deoxygenated by a N_2 stream. The initial solution pH was adjusted by HCl (1.0 mol L^{-1}) or NaOH (1.0 mol L^{-1}). At specific time intervals, samples were withdrawn with the aid of a syringe to analyze the concentration of nitrate, nitrite and ammonia in the solution after filtering it through a 0.22 μm membrane filter. Control experiments without the reductant were also performed at the same conditions. All solutions were prepared using ultrapure water produced by a Millipore-Q system (Millipore Synergy, USA).

As previous studies, N_2 selectivity could be calculated from the balance of nitrogen products analyzed in solution [20,21]. In this study, the off-gas from the reactor was absorbed in acidic solution for analyzing gas phase ammonia, which might has been produced when the solution pH was alkaline. Nitrate and nitrite adsorbed on the composites were detected after being washed using 5 mmol L^{-1} NaOH. Nitrate and nitrite were analyzed by ion chromatography (Dionex 1000, USA) with an AS11-HC guard column using 15 mmol L^{-1} KOH solution as mobile phase at a flow rate of 1.0 mL min^{-1}. Ammonium was determined by a UV–Vis spectrophotometer (UV 2450, Shimadzu, Japan) with the light absorption at 697 nm using salicylic acid spectrophotometry. The solution pH was determined by a pH meter (FE20, Mettler Toledo, Switzerland).

Nitrate removal ($R_{nitrate}$), nitrate conversation ($C_{nitrate}$) and the selectivity of each product ($S_{nitrite}$, $S_{ammonia}$, and $S_{nitrogen}$) were calculated as follows:

$$R_{nitrate}(\%) = \frac{[NO_3^-]_i - [NO_3^-]_f}{[NO_3^-]_i} \times 100 \quad (1)$$

$$C_{nitrate}(\%) = \frac{[NO_3^-]_i - [NO_3^-]_f - [NO_3^-]_a}{[NO_3^-]_i} \times 100 \quad (2)$$

$$S_{nitrite}(\%) = \frac{[NO_2^-]_f + [NO_2^-]_a}{[NO_3^-]_i - [NO_3^-]_f - [NO_3^-]_a} \times 100 \quad (3)$$

$$S_{ammonia}(\%) = \frac{[NH_4^+]_f + [NH_4^+]_a}{[NO_3^-]_i - [NO_3^-]_f - [NO_3^-]_a} \times 100 \quad (4)$$

$$S_{nitrogen}(\%) = \frac{[NO_3^-]_i - [NO_3^-]_f - [NO_3^-]_a - [NO_2^-]_f - [NO_2^-]_a - [NH_4^+]_f + [NH_4^+]_a}{[NO_3^-]_i - [NO_3^-]_f - [NO_3^-]_a} \times 100 = 100 - S_{nitrite}(\%) - S_{ammonia}(\%) \quad (5)$$

where $[NO_3^-]_i$ is the initial amount of NO_3^--N (mg); $[NO_3^-]_f$, $[NO_2^-]_f$ and $[NH_4^+]_f$ are the final amount of NO_3^--N, NO_2^--N and NH_4^+-N (mg) in the solution, respectively; $[NO_3^-]_a$ and $[NO_2^-]_a$ are the amount of NO_3^--N and NO_2^--N (mg) adsorbed on the composites, respectively; $[NH_4^+]_a$ is the amount of NH_4^+-N (mg) absorbed in acidic solution.

3. Results and discussion

3.1. Effect of methods of preparation

Nitrate removal by DOW 3N-Fe/Pd (8 wt.% Fe and 8 wt.% Pd) and DOW 3N-Fe/Pd-R (8 wt.% Fe and 8 wt.% Pd) is shown in Fig. 1. The kinetics of nitrate removal was well fitted to first-order kinetic model.

$$\frac{d[NO_3^-]}{dt} = -k_{obs}[NO_3^-] \quad (6)$$

$$\ln\left(\frac{[NO_3^-]_0}{[NO_3^-]_t}\right) = k_{obs}t \quad (7)$$

where $[NO_3^-]_t$ is the concentration of NO_3^--N (mg L^{-1}) at time t, $[NO_3^-]_0$ is the initial concentration of NO_3^--N (mg L^{-1}), k_{obs} is the observed first-order rate constant (min^{-1}).

The activity and the selectivity of the two composites are summarized in Table 1. The amount of Fe and Pd leached from the composites after NO_3^- reduction were negligible in all experimental runs, indicating that the deactivation of composites due to loss of Fe and Pd was not considered during the reaction. The results in Table 1 clearly show that DOW 3N-Fe/Pd displayed higher removals and conversion efficiencies as compared to DOW 3N-Fe/Pd-R. The 97.8% of nitrate removal was observed with DOW 3N-Fe/Pd at the rate of $0.0156 \pm 0.0006\ min^{-1}$; while a lower nitrate removal (92.0%) was obtained at the rate of $0.0387 \pm 0.0030\ min^{-1}$ using DOW 3N-Fe/Pd-R. Nitrate removal by DOW 3N was also tested and shown in Fig. S1. The removal of nitrate with DOW 3N was much lower than with DOW 3N-Fe/Pd and DOW 3N-Fe/Pd-R. No reduction products (NH_4^+, NO_2^-, etc.) were detected, indicating no contribution of DOW 3N resin to nitrate reduction. In the case of nitrate reduction by DOW 3N-Fe/Pd and DOW 3N-Fe/Pd-R, NH_4^+ was the only detectable stable product and NO_2^- was not detected in the solution. The pH increased rapidly from initial 6.75 to 9.20 at the initial stage, then remained almost unchanged. The concentrations of ammonia for nitrate reduction with DOW 3N-Fe/Pd-R during all the time were always higher than those with DOW 3N-Fe/Pd. The N_2 selectivities of DOW 3N-Fe/Pd-R and DOW 3N-Fe/Pd for nitrate reduction were 47.5% and 69.2%, respectively. The results clearly demonstrate that the preparation method not only affected the activity of Fe–Pd nanoparticles, but also their selectivity.

To understand the different performances of DOW 3N-Fe/Pd and DOW 3N-Fe/Pd-R for nitrate removal, TEM, EDS and XRD analyses were used to assess the morphology and the size of the supported bimetallic nanoparticles. TEM images (Fig. 2) clearly show that Fe/Pd nanoparticles were well dispersed on the surface of DOW 3N and the particles size were mainly between 3 and 5 nm for both DOW 3N-Fe/Pd and DOW 3N-Fe/Pd-R. Moreover, The EDS mappings of the two composites in Fig. 3 showed that both Fe and Pd particles were uniformly distributed on the surface of

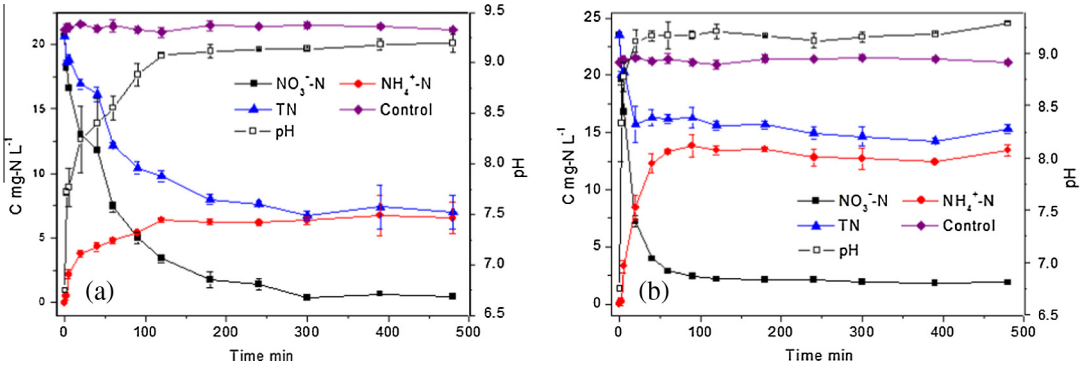

Fig. 1. Concentration of nitrate, ammonium ions, total nitrogen (TN) and pH during a batch test of nitrate reduction by (a) DOW 3N-Fe/Pd and (b) DOW 3N-Fe/Pd-R at the initial pH = 6.75 (with 8 wt.% Fe and 8 wt.% Pd).

Table 1
Results of nitrate removal by supported nanoparticles at different experimental conditions.

Prepared method	Pd loading (wt.%)	Initial pH	$R_{nitrate}$ (%)	$C_{nitrate}$ (%)	$A_{nitrate}$ (wt.%)	$A_{nitrite}$ (wt.%)	S_{N2} (%)
DOW 3N-Fe/Pd-R	8	6.75	92.0	91.0	1.29	–	47.5
DOW 3N-Fe/Pd	2	6.75	99.2	75.5	1.42	–	36.8
DOW 3N-Fe/Pd	4	6.75	98.2	78.5	2.85	0.32	56.9
DOW 3N-Fe/Pd	6	6.75	98.5	83.4	3.59	0.14	68.2
DOW 3N-Fe/Pd	8	6.75	97.8	86.0	3.13	0.63	69.2
DOW 3N-Fe/Pd	8	5.31	95.7	85.1	7.76	0.49	61.4
DOW 3N-Fe/Pd	8	8.67	96.1	78.4	10.46	1.77	71.0

$R_{nitrate}$: the removal efficiency of nitrate; $C_{nitrate}$: the conversation of nitrate; S_{N2}: the selectivity of nitrogen gas; $A_{nitrate}$ and $A_{nitrite}$: the adsorption of NO_3^--N and NO_2^--N (mg) on the composites, respectively, which was calculated by the ratio of the adsorption amount of NO_3^--N and NO_2^--N to the initial amount of NO_3^--N (mg).

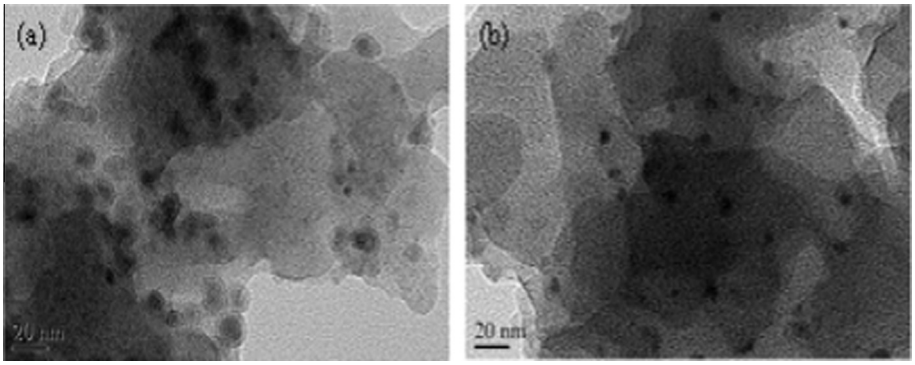

Fig. 2. TEM images and size distribution of the supported nanoparticles: (a) DOW 3N-Fe/Pd-R and (b) DOW 3N-Fe/Pd.

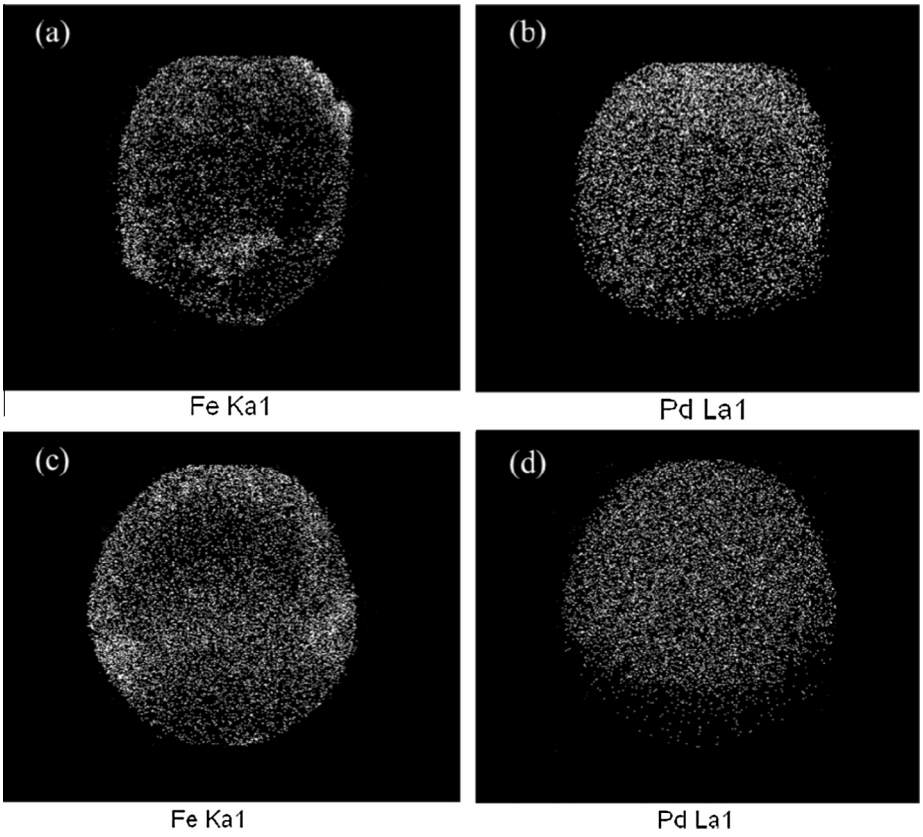

Fig. 3. Energy dispersive X-ray spectroscopy (EDS) of DOW 3N-Fe/Pd (a,b) and DOW 3N-Fe/Pd-R (c,d).

DOW 3N, indicating that DOW 3N provided the suitable surface environment for the dense and uniform deposition of Fe and Pd particles. Therefore, both of the supported Fe/Pd bimetallic nanoparticles prepared using two different methods exhibited high nitrate removal (>90%).

TEM images in Fig. 2 reveal a visible oxidized layer on the surface of the nanoparticles of DOW 3N-Fe/Pd-R; while it is not evident on that of DOW 3N-Fe/Pd. The oxidized layer not only lowered the reduction activity of nanoparticles for nitrate, but also deactivated Pd nanoparticles and inhibited the adsorption of atomic hydrogen on active sites of Pd surface, resulting in the decrease of N_2 selectivity.

DOW 3N-Fe/Pd and DOW 3N-Fe/Pd-R were also characterized by X-ray diffraction (shown in Fig. S2). No clear sign of Fe was observed for both samples, probably because iron nanoparticles were amorphous. DOW 3N-Fe/Pd showed wide diffraction signal at 40°, which can be assigned to Pd^0. However, no peaks at 40° were detected for DOW 3N-Fe/Pd-R, indicating the presence of amorphous or poorly crystalline Pd nanoparticles. The results indicate that better Pd^0 crystal contributed to higher N_2 selectivity with the supported Fe–Pd nanoparticles.

To elucidate in detail how Pd loading and solution pH affected the activity and the selectivity of the supported Fe–Pd nanoparticles, additional experiments focused only on DOW 3N-Fe/Pd, because its nitrate removal and N_2 selectivity were superior to those of DOW 3N-Fe/Pd-R.

3.2. Effect of Pd loading

The Pd/Fe ratio on DOW 3N surface is crucial for the reduction properties of DOW 3N-Fe/Pd. In this study, the amount of Fe on DOW 3N was fixed at 8 wt.% and variations of Pd loadings (2, 4,

6, and 8 wt.%) were used to assess the nitrate removal and N_2 selectivity at initial pH 6.75. The nitrate removal at four different levels of Pd loading is depicted in Fig. 4. Table 1 presents the nitrate removal efficiencies and transformation product selectivities. It is clearly seen in Table 1 that all experimental cases showed basically the identical nitrate removal efficiency and removal rate constant k_{obs} (0.0188 ± 0.0013, 0.0186 ± 0.0005, 0.0181 ± 0.0005 and 0.0156 ± 0.0006 min^{-1} at the 2%, 4%, 6–8% of Pd loading, respectively). The results indicate that the Pd loading had the negligible influence on nitrate removal. The same Fe loading and similar nanoparticles size (shown in Fig. S3) may be responsible for similar nitrate removal efficiency and rate constant k_{obs}. In addition, we

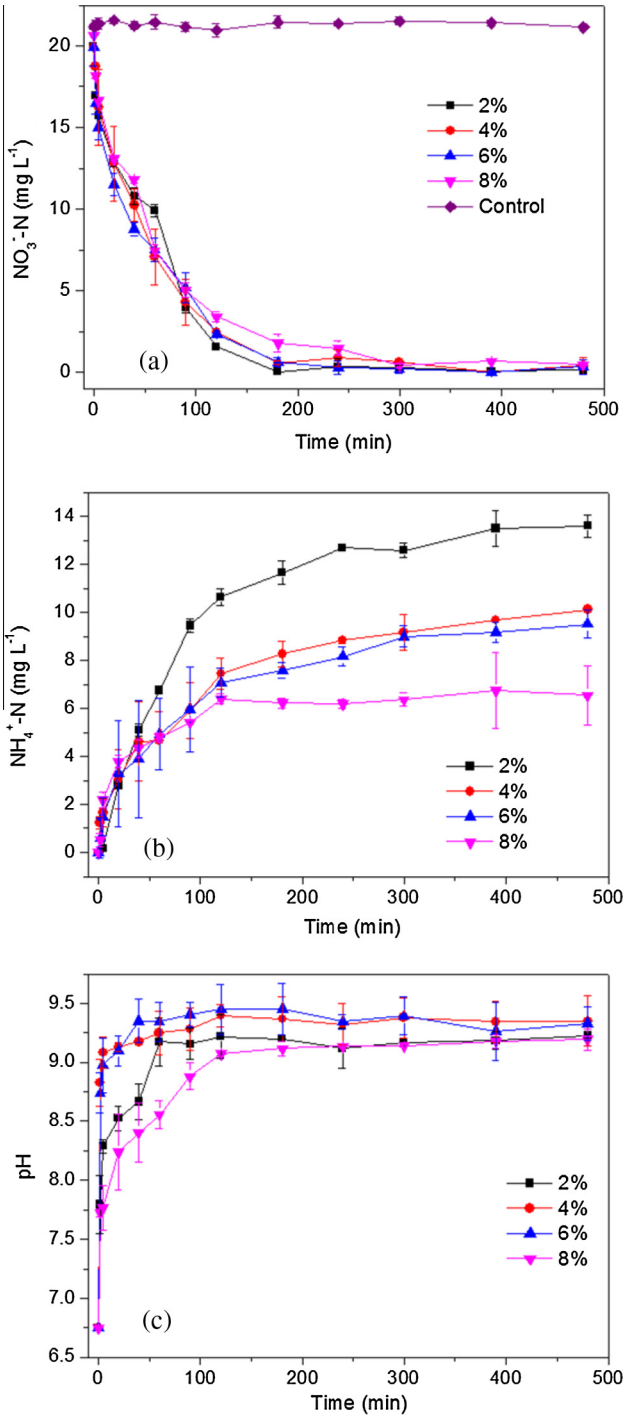

Fig. 4. Removal of nitrate by DOW 3N-Fe/Pd with different Pd loading: (a) NO_3^--N, (b) NH_4^+-N and (c) pH variation.

observed that $C_{nitrate}$ was much lower than the removal efficiency of nitrate. The possible reason is that some NO_3^- was adsorbed onto the resin or the metallic oxide formed during the reaction. In contrast to nitrate removal, the amount of ammonium was found to decrease with increasing Pd loading. Therefore, nitrogen gas selectivity increased from 36.8% to 68.2% as Pd loading increased from 2 wt.% to 6 wt.% (shown in Table 1). But, with further increase in the Pd content, a minor increase in nitrogen gas selectivity was observed. The highest nitrogen gas selectivity (69.2%) was obtained at 8 wt.% of Pd loading.

The reduction of NO_3^- by bimetallic Fe/Pd nanoparticles can be considered as a consecutive reaction through NO_2^- as an intermediate product. Nitrate was firstly reduced to nitrite; then nitrite was readsorbed at the Pd surface to be further converted to ammonium or nitrogen gas by atomic hydrogen adsorbed on active sites of Pd surface [2,22]. It has been known that the activated hydrogen adsorbed on the active sites of Pd particles can abstract oxygen from nitrite, and then two nitrogen atoms are consecutively bonded to form nitrogen gas [23]. Thus the amount of hydrogen is an important fact for the N_2 selectivity. In the bimetallic Fe/Pd materials, the adsorbed hydrogen was formed on the Pd surface. When the Pd loading was increased, the concentration of atomic hydrogen adsorbed on active sites of Pd surface was increased, resulting in the enhancement of nitrogen gas selectivity. Moreover, it was reported that there were various kinds of Pd sites with different coordinative unsaturation at the surface of Pd particles, which exhibited different selectivities. The edge and corner sites of Pd possessed higher abilities for hydrogenation and were probably favorable for the formation of NH_3; on the contrary, N_2 would be favorably formed on the terrace sites of the Pd crystallites [24,25]. In this study, as Pd loading increased, the probability of direct contact between Fe atoms and Pd atoms also increased. Therefore, the fraction of edge or corner Pd sites, which were effective for NH_3 formation, would decrease with the increase of Pd loading, resulting in higher nitrogen gas selectivity.

3.3. Effect of pH value

The pH dependence of nitrate removal activity and ammonium formation for DOW 3N-Fe/Pd (8 wt.% Fe and 8 wt.% Pd) is displayed in Fig. 5. The NO_2^- was not detected throughout the experiment. At various pH levels (pH = 5.31–8.67), the solution pH experienced a rapid rise within 40 min of the reaction (Fig. 5c) and then a much slower increase to about 9.3. The k_{obs} values of nitrate reduction at pH = 5.31, 6.75 and 8.67 were 0.0196 ± 0.0006, 0.0156 ± 0.0006 and 0.0120 ± 0.0004 min^{-1}, respectively, manifesting that high pH value had a negative effect on the k_{obs} value. The faster nitrate reduction at lower pH was attributed to the greater production of H_2, which in turn refreshed the surface reactivity of the nanoparticles [14]. In all cases, although lower pH enhanced the nitrate removal rate, the removal efficiency of nitrate kept basically constant. However, a negative effect of high pH value on the NO_3^- conversion was observed, in which the value dropped obviously at pH 8.67. This is most likely due to H^+ consumption during the reactions. Furthermore, the formation of ferrous hydroxide at pH 8.67 may block reactive sites on the Fe/Pd surface, and then inhibit the conversion of nitrate.

We know from Table 1 that the N_2 selectivity increased with an increase of pH value, and the maximum N_2 selectivity (71.0%) was achieved at pH value of 8.67. It was reported that for nitrate reduction by ZVI or iron-based bimetallic nanoparticles, nitrate was first reduced to nitrite as an intermediate product, and then nitrite was converted to nitrogen and ammonia. Therefore, the hydrogenation of NO_2^- is a key step in determining selectivity to N_2. Previous investigations had demonstrated that increasing the nitrite-to-hydrogen ratio resulted in the decrease of ammonia selectivity

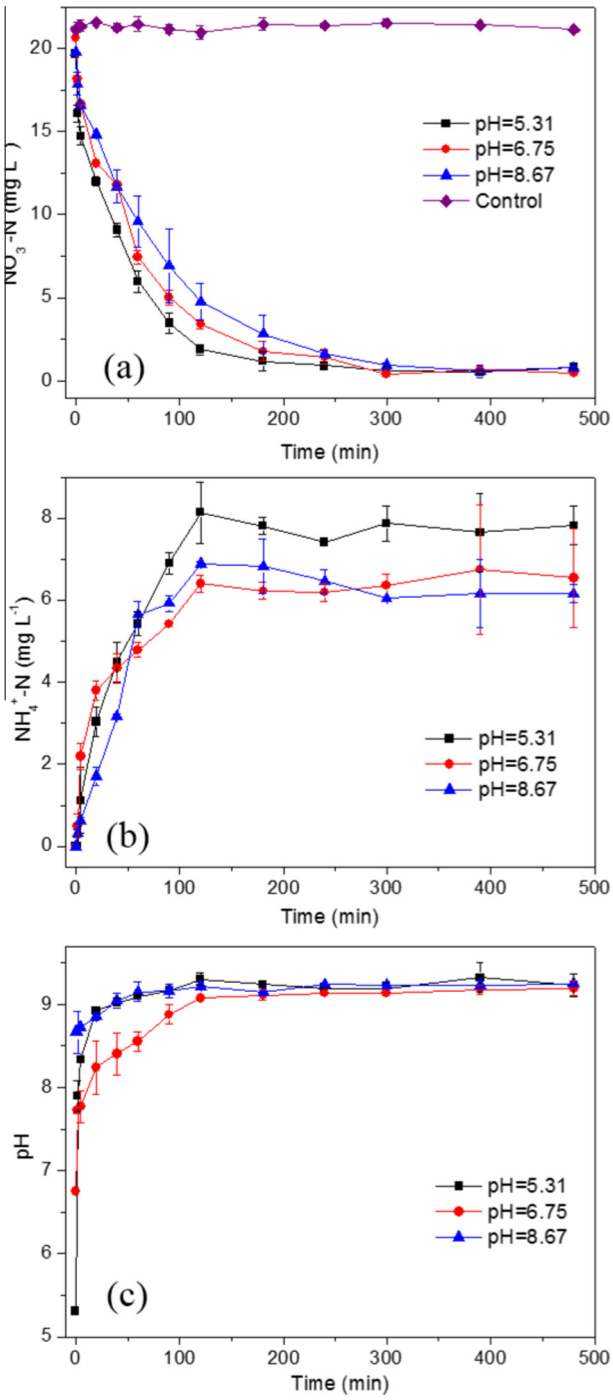

Fig. 5. Removal of nitrate by DOW 3N-Fe/Pd (8 wt.% Fe and 8 wt.% Pd) with different initial pH value: (a) NO_3^--N, (b) NH_4^+-N and (c) pH variation.

[2,22–25]. As shown in Table 1, the surface concentration of nitrite at pH 8.67 was the highest. Therefore, although higher pH value would reduce the formation of the adsorbed hydrogen on the surface of Pd, it could result in an increase in the ratio of the surface concentrations of nitrite and hydrogen, and thus promoted the production of N_2. The result is in agreement with observations by Liou et al. [13,26].

3.4. Nitrate removal mechanism

The nitrate removal by DOW 3N-Fe/Pd was verified by the experimental results of adsorption on the DOW 3N and reduction by bimetallic Fe/Pd nanoparticles. Compared with monometallic Fe nanoparticles supported on DOW 3N (shown in Fig. S4), bimetallic Fe/Pd nanoparticles supported on DOW 3N had much higher reactivity and reduction rate for NO_3^-, confirming that the addition of a second metal (Pd) significantly enhanced the reactivity of Fe for nitrate reduction. The possible reason is as follows. In the bimetallic Fe/Pd nanoparticle system, the galvanic couple can be formed between Fe and Pd [18]. The Fe functions as the anode where oxidation of Fe(0) to Fe(II) occurs; while Pd serves as the cathode at which the reduction of nitrate to nitrite takes place (Eqs. (8) and (9)). Galvanic coupling between Fe and Pd accelerates the oxidization of Fe(0) and increases the rate of electron transfer to nitrate, resulting in higher reduction rate for NO_3^- than monometallic Fe nanoparticles. It also favors water reduction and formation of activated H-species [8], which in turn could contribute to the increased rates of nitrate reduction. Furthermore, as iron is corroded, protons from water can be reduced to atomic H at the Pd surface (Eq. (10)) [27]. At the same time, protons from water can be reduced to atomic H at Fe surface and then to molecular hydrogen (Eq. (11)); the hydrogen is adsorbed to the palladium lattice where it is partially dissociated back to atomic hydrogen (Eq. (12)). Atomic hydrogen, a powerful reductant, abstracts the oxygen of NO_2^- reabsorbed on Pd surface into the end product N_2 and NH_3 (Eqs. (13) and (14)) [2].

$$Fe^0 \rightarrow 2e^- + Fe^{2+} \quad (8)$$

$$NO_3^-(aq) + 2e^- + H_2O(l) \rightarrow NO_3^-(aq) + 2OH^-(aq) \quad (9)$$

$$H_2O + e^- \rightarrow OH^- + H_{ads} \quad (10)$$

$$H_{ads} + H_{ads} \rightarrow H_2 \quad (11)$$

$$H_2 \xrightarrow{Pd} 2H_{ads} \quad (12)$$

$$2NO_2^- + 4H_{ads} - Pd(0) \rightarrow Pd(0) + N_2 + 2OH^- \quad (13)$$

$$2NO_2^- + 12H_{ads} - Pd(0) \rightarrow Pd(0) + 2NH_4^+ + 4OH^- \quad (14)$$

In order to better understand the nitrate reduction mechanism, DOW 3N-Fe/Pd (8 wt.% Fe and 8 wt.% Pd) was analyzed by XPS before and after the nitrate reduction (Fig. 6). No peak of Fe^0 is observed in Fig. 6(a), which is mainly due to a layer of oxide film on the surface of the nanoparticles giving rise to a broad signal. The Fe2p peaks at binding energies of 709 eV and 723 eV are assigned to oxidized iron. The surface composition of Fe(II) increased by 59.3% after the reaction, indicating that Fe(0) was oxidized to Fe(II). Fig. 6 (b) shows that two peaks at 336 eV and 340 eV (Pd^0) were observed before the reduction; after that, Pd^0 as well as its oxidized state-Pd(II) (binding energy of 338 eV and 343 eV) were also detected. This observation is consistent with the study of Barrabés et al. [28]. The partial re-oxidation from Pd^0 to Pd(II) during the reaction substantiated the participation of the catalytic Pd as an active site. Therefore, based on the XPS analysis, the redox reaction between nitrite ions and Pd^0 occurred, leading to the formation of oxidized of Pd.

In this study, as much as 71.0% N_2 selectivity was obtained in the reduction of aqueous nitrate using bimetallic Fe–Pd nanoparticles supported on DOW 3N, which is the highest value for the nitrate reduction at similar conditions among other reports thus far. The surface chemistry and pore structure of the support DOW 3N resin might play an important role on the high N_2 selectivity. The influence of internal mass transfer limitations inside the support on the activity and selectivity of nitrate reduction has been confirmed by some studies [25,29]. The severe transport limitations of NO_3^- and NO_2^- inside the pore of supports could lower

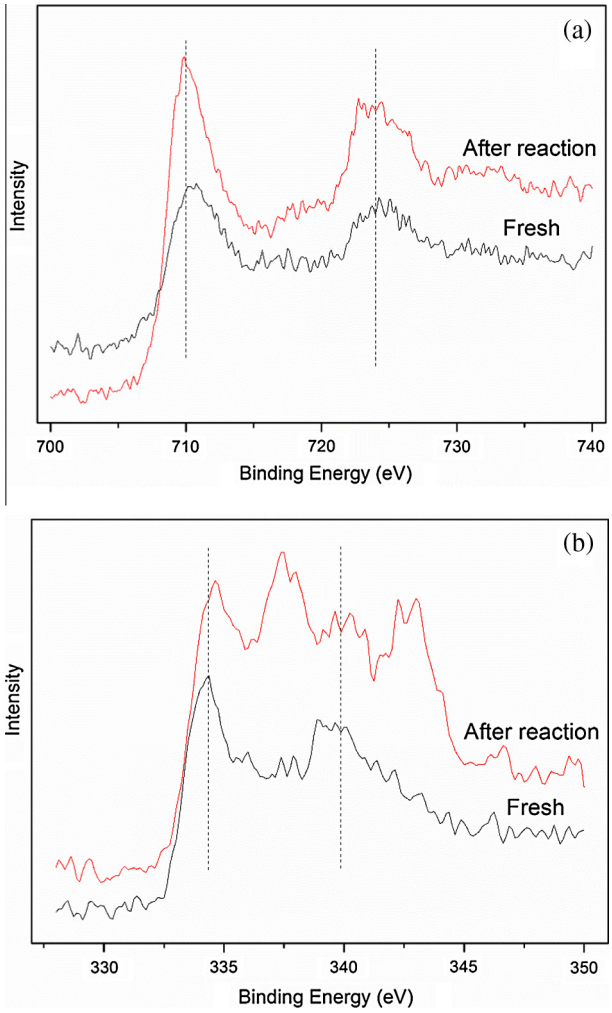

Fig. 6. XPS signals of (a) Fe2p and (b) Pd3d on the surface of DOW 3N-Fe/Pd (with 8 wt.% Fe and 8 wt.% Pd) before and after the reaction.

the activity and the selectivity of nitrate reduction. In this study, DOW 3N (DOWEX™ M4195) is composed of a polystyrene cross-linked with divinyl benzene backbone and bis (2-pyridylmethyl) amine functional groups. Due to the non-existence of charged functional groups fixed on the matrix of DOW 3N, NO_3^- can permeate into the polymer phase of DOW 3N by diffusion without Donnan exclusion effect. Moreover, DOW 3N-Fe/Pd possesses high mesoporous volume and low microporosity (shown in Fig. S5). Therefore, the internal mass transfer limitation towards nitrate was minimized. In addition, DOW 3N kept good adsorption capacities for nitrate at various pH (shown in Fig. S1). The study of Mikami et al. [22] has shown that high NO_3^- concentration favored selectivity for N_2 over NH_4^+. Therefore, due to the decrease of mass transfer limitations and high adsorption capacity of nitrate, more nitrates may be reduced to nitrite and accumulated at reactive Pd sites, resulting in a higher nitrite to hydrogen ratio and the promotion of N—N pairing. The EDS mappings of DOW 3N-Fe/Pd (8 wt.% Fe and 8 wt.% Pd) in Fig. 3 clearly showed that both Fe and Pd particles were uniformly distributed on the surface of DOW-3N. This fact indicates that the support DOW 3N minimized the negative aggregation of nanoparticles and promoted the uniform distribution of Fe and Pd particles. A closer contact distance between Pd and Fe on the surface of DOW 3N-Fe/Pd could result in a low density of low coordination sites (i.e., edges and corners), which were effective for NH_3 formation. Therefore, higher N_2 selectivity was achieved due to more terrace Pd sites with high coordination [25].

4. Conclusions

The preparation method affected the activity and selectivity of the bimetallic Fe–Pd nanoparticles supported on chelating resin DOW 3N. The results show that DOW 3N-Fe/Pd with no oxidized layer and better Pd^0 crystal presented better performance than DOW 3N-Fe/Pd-R. The Pd content and solution pH seemed to affect significantly the performance of the supported bimetallic nanoparticles. Increasing the Pd content and solution pH can improve the selectivity to N_2. DOW 3N-Fe/Pd with 8 wt.% Pd–8 wt.% Fe showed the highest selectivity to N_2 (71.0%) when the solution pH was 8.67.

Acknowledgments

This research was financially funded by the Major Science and Technology Program for Water Pollution Control and Treatment (Grant No. 2012ZX07101-003) and the State Key Program of National Natural Science of China (No. 51438008).

Appendix A. Supplementary data

Supplementary data associated with this article can be found, in the online version, at http://dx.doi.org/10.1016/j.cej.2015.10.054.

References

[1] C. Della Rocca, V. Belgiorno, S. Meric, Heterotrophic/autotrophic denitrification (HAD) of drinking water: prospective use for permeable reactive barrier, Desalination 210 (2007) 194–204.
[2] U. Prüsse, K.D. Vorlop, Supported bimetallic palladium catalysts for water-phase nitrate reduction, J. Mol. Catal. A: Chem. 173 (2001) 313–328.
[3] G.C.C. Yang, H.L. Lee, Chemical reduction of nitrate by nanosized iron: kinetics and pathways, Water Res. 39 (2005) 884–894.
[4] K. Sohn, S.W. Kang, S. Ahn, M. Woo, S. Yang, Fe(0) nanoparticles for nitrate reduction: stability, reactivity, and transformation, Environ. Sci. Technol. 40 (2006) 5514–5519.
[5] Y. Hwang, D. Kim, H. Shin, Mechanism study of nitrate reduction by nano zero valent iron, J. Hazard. Mater. 185 (2011) 1513–1521.
[6] A. Ryu, S.-W. Jeong, A. Jang, H. Choi, Reduction of highly concentrated nitrate using nanoscale zero-valent iron: effects of aggregation and catalyst on reactivity, Appl. Catal. B: Environ. 105 (2011) 128–135.
[7] H. Song, B.-H. Jeon, C.-M. Chon, Y. Kim, I.-H. Nam, F.W. Schwartz, D.-W. Cho, The effect of granular ferric hydroxide amendment on the reduction of nitrate in groundwater by zero-valent iron, Chemosphere 93 (2013) 2767–2773.
[8] H.-S. Kim, T. Kim, J.-Y. Ahn, K.-Y. Hwang, J.-Y. Park, T.-T. Lim, I. Hwang, Aging characteristics and reactivity of two types of nanoscale zero-valent iron particles (Fe^{BH} and Fe^{H2}) in nitrate reduction, Chem. Eng. J. 197 (2012) 16–23.
[9] Y. Zhang, Y. Li, J. Li, L. Hu, X. Zheng, Enhanced removal of nitrate by a novel composite: nanoscale zero valent iron supported on pillared clay, Chem. Eng. J. 171 (2011) 526–531.
[10] O.S.G.P. Soares, J.J.M. Orfao, M.F.R. Pereira, Activated carbon supported metal catalysts for nitrate and nitrite reduction in water, Catal. Lett. 126 (2008) 253–260.
[11] S. Mossa, B. Hosseini, M. Ataie-Ashtiani, Kholghi, nitrate reduction by nano-Fe/Cu particles in packed column, Desalination 276 (2011) 214–221.
[12] Y.H. Liou, S.L. Lo, C.J. Lin, W.H. Kuan, S.C. Weng, Chemical reduction of an unbuffered nitrate solution using catalyzed and uncatalyzed nanoscale iron particles, J. Hazard. Mater. 127 (2005) 102–110.
[13] Y.H. Liou, C.J. Lin, S.C. Weng, H.H. Ou, S.L. Lo, Selective decomposition of aqueous nitrate into nitrogen using iron deposited bimetals, Environ. Sci. Technol. 43 (2009) 2482–2488.
[14] Z. Xiong, D. Zhao, G. Pan, Rapid and controlled transformation of nitrate in water and brine by stabilized iron nanoparticles, J. Nanopart. Res. 11 (2009) 807–819.
[15] C. Noubactep, Comments on "Mechanism study of nitrate reduction by nano zero valent iron" by Hwang et al. [J. Hazard. Mater. (2010), doi:10.1016/j.jhazmat.2010.10.078], J. Hazard. Mater. 186 (2011) 946–947.
[16] J. Shi, S. Yi, H. He, C. Long, A. Li, Preparation of nanoscale zero-valent iron supported on chelating resin with nitrogen donor atoms for simultaneous reduction of Pb^{2+} and NO_3^-, Chem. Eng. J. 230 (2013) 166–171.
[17] F. He, D. Zhao, Hydrodechlorination of trichloroethene using stabilized Fe–Pd nanoparticles: reaction mechanism and effects of stabilizers, catalysts and reaction conditions, Appl. Catal. B: Environ. 84 (2008) 533–540.
[18] Y. Xie, D.M. Cwiertny, Chlorinated solvent transformation by palladized zerovalent iron: mechanistic insights from reductant loading studies and solvent kinetic isotope effects, Environ. Sci. Technol. 47 (2013) 7940–7948.

[19] M.S. Wong, P.J.J. Alvarez, Y.-L. Fang, N. Akçin, M.O. Nutt, J.T. Miller, K.N. Heck, Cleaner water using bimetallic nanoparticle catalysts, J. Chem. Technol. Biot. 84 (2009) 158–166.
[20] H.T. Ren, S.Y. Jia, J.J. Zou, S.H. Wu, X. Han, A facile preparation of Ag_2O/P25 photocatalyst for selective reduction of nitrate, Appl. Catal. B: Environ. 176–177 (2015) 53–61.
[21] M. Al Bahri, L. Calvo, M.A. Gilarranz, J.J. Rodriguez, F. Epron, Activated carbon supported metal catalysts for reduction of nitrate in water with high selectivity towards N2, Appl. Catal. B: Environ. 138 (139) (2013) 141–148.
[22] I. Mikami, Y. Sakamoto, Y. Yoshinaga, T. Okuhara, Kinetic and adsorption studies on the hydrogenation of nitrate and nitrite in water using Pd–Cu on active carbon support, Appl. Catal. B: Environ. 44 (2003) 79–86.
[23] K.A. Guy, H. Xu, J.C. Yang, C.J. Werth, J.R. Shapley, Catalytic nitrate and nitrite reduction with Pd–Cu/PVP colloids in water: composition, structure, and reactivity correlations, J. Phys. Chem. C 113 (2009) 8177–8185.
[24] Y. Yoshinaga, T. Akita, I. Mikami, T. Okuhara, Hydrogenation of nitrate in water to nitrogen over Pd–Cu supported on active carbon, J. Catal. 207 (2002) 37–45.
[25] D. Shuai, J.K. Choe, J.R. Shapley, C.J. Werth, Enhanced activity and selectivity of carbon nanofiber supported Pd catalysts for nitrite reduction, Environ. Sci. Technol. 46 (2012) 2847–2855.
[26] Y.H. Liou, C.J. Lin, I.C. Hung, S.Y. Chen, S.L. Lo, Selective reduction of NO_3^- to N_2 with bimetallic particles of Zn coupled with palladium, platinum, and copper, Chem. Eng. J. 181–182 (2012) 236–242.
[27] B.P. Chaplin, M. Reinhard, W.F. Schneider, Critical review of Pd-based catalytic treatment of priority contaminants in water, Environ. Sci. Technol. 46 (2012) 3655–3670.
[28] N. Barrabés, J. Just, A. Dafinov, F. Medina, J.L.G. Fierro, J.E. Sueiras, P. Salagre, Y. Cesteros, Catalytic reduction of nitrate on Pt–Cu and Pd–Cu on active carbon using continuous reactor: the effect of copper nanoparticles, Appl. Catal. B: Environ. 62 (2006) 77–85.
[29] D. Gasparovicova, M. Kralik, M. Hronec, A. Biffis, M. Zecca, B. Corain, Reduction of nitrates dissolved in water over palladium-copper catalysts supported on a strong cationic resin, J. Mol. Catal. A: Chem. 244 (2006) 258–266.